Epitaxial Growth Mechanism for Perovskite Oxide Thin Films under Pulsed Laser Irradiation in Chemical Solution Deposition Process

Tomohiko Nakajima,*,† Tetsuo Tsuchiya,† Masaki Ichihara,‡ Hideaki Nagai,† and Toshiya Kumagai†

National Institute of Advanced Industrial Science and Technology, Tsukuba Central 5, 1-1-1 Higashi, Tsukuba, Ibaraki 305-8565, Japan, and Materials Design and Characterization Laboratory, Institute for Solid State Physics, University of Tokyo, 5-1-5 Kashiwanoha, Kashiwa, Chiba 277-8581, Japan

Received July 2, 2008. Revised Manuscript Received September 24, 2008

We have studied the epitaxial growth of perovskite manganite $LaMnO_3$ (LMO) on $SrTiO_3(100)$ and $LaAlO_3(100)$ substrates by means of chemical solution deposition assisted by pulsed UV laser irradiation, termed excimer laser-assisted metal organic deposition (ELAMOD). Cross-sectional transmission electron microscopy observations revealed that the LMO was crystallized from a coated amorphous LMO matrix by the pulsed laser irradiation, and was preferentially grown from the substrate surface. In this process, the optical absorbance of the substrate for the irradiated laser plays an essential role for starting the epitaxial growth. This indicates a photochemical effect due to the UV laser irradiation; the photochemically activated growth interface strongly enhanced chemical bond formation, leading to epitaxial growth of LMO. The film temperature under the excimer laser irradiation was estimated using theoretical simulations with a one-dimensional heat equation, and it was found to increase to about 1000−1800 °C for 90 ns. The photothermal temperature rise contributes to ion-migration for crystallization, and furthers the rapid epitaxial growth initiated by the photochemical effect. Thus, the photochemical and photothermal effects are considered to assume the roles of initiator and enhancer of epitaxial growth under the laser irradiation in the ELAMOD process.

Introduction

A large number of inorganic materials have been investigated for future electronics devices. In particular, many researchers have focused on oxide materials that demonstrate fascinating electrical, magnetic, and optical properties. In many cases, oxide materials are incorporated in electronic devices as thin films. There are two main requirements for film growth methods for future applications: (1) efficient fabrication for lower cost, and (2) low-temperature operation for substrates that cannot withstand high temperatures ($T >$ 500 °C). It is now widely accepted that chemical solution deposition (CSD) methods, such as a metal organic deposition (MOD)[1,2] and sol−gel[3,4] processes are better than physical and chemical vapor deposition processes in terms of process simplicity and low cost. However, the application of CSD as a conventional heating process is also a big issue for low-temperature fabrication and is generally limited by the heat resistance properties of the substrate.

To resolve this problem, our research group as well as others have investigated new processes by means of a combination of CSD and ultraviolet (UV) irradiation.[5−8] We have investigated a new method to fabricate oxide thin films at low temperatures using an advanced conventional MOD process, wherein oxide films are crystallized by means of excimer laser irradiation ($\lambda = 193$, 248, and 308 nm) instead of high-temperature furnace heating in the MOD process.[9−12] We have named this process excimer laser-assisted metal organic deposition (ELAMOD). Thus far, we have demonstrated that not only polycrystalline films but also epitaxial films of oxide materials can be grown by ELAMOD, when a single-crystal substrate has a small lattice mismatch with the film.[9,12] In these studies, we noticed that crystal growth

* Corresponding author. E-mail: t-nakajima@aist.go.jp.
† National Institute of Advanced Industrial Science and Technology.
‡ University of Tokyo.

(1) Westerheim, A. C.; Mcintyre, P. C.; Basu, S. N.; Bhatt, D.; Yujahnes, L. S.; Anderson, A. C.; Cima, M. J. *J. Electron. Mater.* **1993**, *22*, 1113.
(2) Mihara, T.; Yoshimori, H.; Watanabe, H.; Araujo, C. A. P. *Jpn. J. Appl. Phys.* **1995**, *34*, 5233.
(3) Avnir, D; Kaufman, V. R.; Reisfeld, R. *J. Non-Cryst. Solids* **1985**, *74*, 395.
(4) Brinker, C. J.; Hurd, A. J.; Frye, G. C. *J. Non-Cryst. Solids* **1990**, *121*, 294.
(5) Nagase, T.; Ooie, T.; Sakakibara, J. *Thin Solid Films* **1999**, *357*, 151.
(6) Tsuchiya, T.; Watanabe, A.; Imai, Y.; Niino, H.; Yamaguchi, I.; Manabe, T.; Kumagai, T.; Mizuta, S. *Jpn. J. Appl. Phys.* **1999**, *38*, L823.
(7) Lai, S. C.; Lue, H-T.; Hsieh, K. Y.; Lung, S. L.; Liu, R.; Wu, T. B.; Donohue, P. P.; Rumsby, P. *J. Appl. Phys.* **2004**, *96*, 2779.
(8) Sandu, C. S.; Teodorescu, V. S.; Ghica, C.; Canut, B.; Blanchin, M. G.; Roger, J. A.; Brioude, A.; Bret, T.; Hoffman, P.; Garapon, C. *Appl. Surf. Sci.* **2003**, *208−209*, 382.
(9) Tsuchiya, T.; Yoshitake, T.; Shimakawa, Y.; Yamaguchi, I.; Manabe, T.; Kumagai, T.; Kubo, Y.; Mizuta, S. *Jpn. J. Appl. Phys.* **2003**, *42*, L956.
(10) Nakajima, T.; Tsuchiya, T.; Kumagai, T. *Jpn. J. Appl. Phys.* **2007**, *46*, L365.
(11) Nakajima, T.; Tsuchiya, T.; Daoudi, K.; Ichihara, M.; Ueda, Y.; Kumagai, T. *Chem. Mater.* **2007**, *19*, 5355.
(12) Daoudi, K.; Tsuchiya, T.; Kumagai, T. *Appl. Phys. A: Mater. Sci. Process.* **2007**, *88*, 639.

10.1021/cm801803g CCC: $40.75
Published on Web 11/07/2008

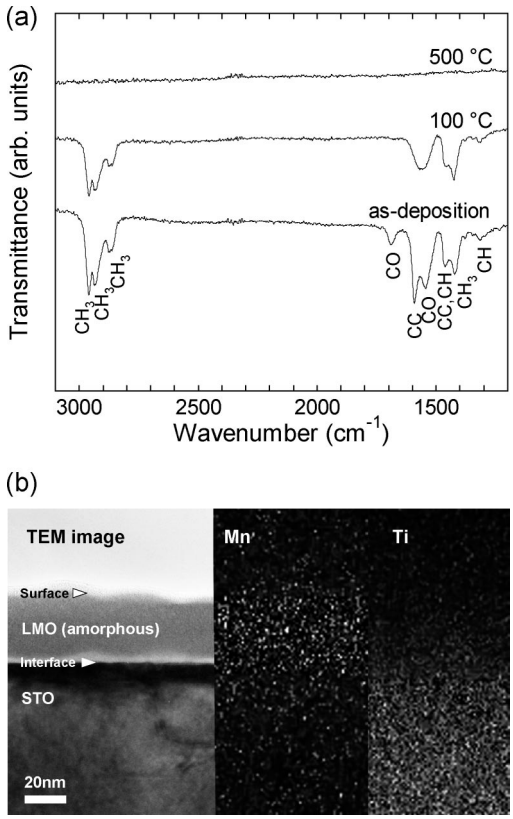

Figure 1. (a) FT-IR spectra for the film as deposited and the films after preheating at 100 and 500 °C. (b) XTEM image of the amorphous LMO film on STO(100) after preheating at 500 °C, and EDX element mapping images of Mn and La.

of oxide films under UV laser irradiation in the CSD process cannot be interpreted by only a photothermal heating effect:[7,15] some photochemical reaction at growth interface should be taken into account to the crystal growth mechanism in this process.[13,14]

In this study, we have therefore investigated the detailed mechanism of epitaxial growth for oxide thin films on single-crystal substrates in the ELAMOD process. The binary oxides such as SnO_2 and TiO_2 can be crystallized from very low temperature at below 500 °C by a heating process, hence, it is difficult to separate the photothermal and photochemical effects. On the other hand, perovskite $LaMnO_3$ (LMO) which has relatively high crystallization temperature at above 800 °C would make easy to understand the difference between them. Therefore, we chose LMO as the target material in this work, and we attempted epitaxial growth of this material on perovskites $SrTiO_3$(100) (STO(100)) and $LaAlO_3$(100) (LAO(100)), both of which have small lattice mismatch with LMO. The epitaxial growth of LMO in ELAMOD is first compared with that in the conventional heating process (MOD) to evaluate the heating effect for crystal growth. Photothermal and photochemical effects for the epitaxial growth of LMO in the ELAMOD process are then discussed for understanding the mechanism on the basis of the experimental results as well as theoretical thermal simulations under pulsed laser irradiation.

Experimental Section

Fabrication Procedure. LMO thin films were fabricated by the MOD and ELAMOD processes. The starting solutions for the LMO films were prepared by mixing 2-ethylhexanoate solutions of the constituent metals diluted with toluene to obtain the required concentration and viscosity for spin-coating. The La:Mn molar ratio in the coating solution was 1.0:1.0. This solution was spin-coated onto STO(100) and LAO(100) substrates at 4000 rpm for 10 s. The coated films were dried at 100 °C in air to remove the solvent, and then preheated to 500 °C in air for 10 min to decompose the organic components of the films. In the ELAMOD process, the films after spin coating and preheating were irradiated with KrF or ArF lasers (Lambda Physik Compex110 and Compex102) at a fluence of 100 mJ/cm^2, and a pulse duration of 26 ns (KrF) and 24 ns (ArF) at 500 and 20 °C in air. The laser energy was homogenized by a beam homogenizer for a 5 × 5 mm^2 area. LMO thin films were also prepared by the conventional MOD process for comparison with ELAMOD; the preheated films were fired at 900 °C in a tube furnace in air for 60−3600 s, and the films were then quenched to room temperature.

The residual organic components of the metal-organic and/or amorphous LMO films were analyzed by Fourier transform infrared spectroscopy (FT-IR) monitored by a Perkin-Elmer spectrum. The crystal growth process and epitaxy of the thin films were observed by cross-sectional transmission electron microscopy (XTEM) using a JEM-2010 (JEOL) instrument operating at 200 kV with an energy -dispersive X-ray spectrometer (EDX). The epitaxial thickness was estimated from the values of 40 points in each sample. The samples for the XTEM observations were prepared by Ar milling using an ion milling device, the BAL-TEC RES100. The thermal conductivity of the amorphous LMO was measured by the hot disk technique.

Theoretical Simulation. Temperature variations during the laser irradiation process can be described by the heat diffusion equation simplified into one-dimensional heat flow, as below[16]

$$\rho C\frac{\partial T}{\partial t} = \kappa\frac{\partial^2 T}{\partial z^2} + \alpha I(z,t) \tag{1}$$

where T is the temperature function at time t and depth z, ρ is the mass density, C is the specific heat capacity, α is the optical absorption coefficient, κ is the thermal conductivity, and $I(z, t)$ is the laser power density. The laser power $I(z, t)$ is given by:

$$I(z,t) = I_0(t)(1-R)\exp(-\alpha z) \tag{2}$$

where R is the reflectance. In the calculation, a contribution of incremental absorbance for the films due to the reflectance at substrate surface was also included to the laser power distribution. $I_0(t)$ is described as a smooth pulse approximated by

$$I_0(t) = I_0\left(\frac{t}{\tau}\right)^{\beta}\exp\left(\beta\left(1-\frac{t}{\tau}\right)\right) \tag{3}$$

where I_0 is the incident pulse power density, τ is the pulse duration, and β determines the temporal pulse shape. We carried out numerical simulations for the temperature variation for the excimer laser irradiation process using a difference approximation based on the above equations. The boundary conditions used were T = 500 or 20 °C at $t = 0$ s (the initial substrate temperature), $T = 500$

(13) Tsuchiya, T.; Daoudi, K.; Manabe, T.; Yamaguchi, I.; Kumagai, T. *Appl. Surf. Sci.* **2007**, *253*, 6504.
(14) Tsuchiya, T.; Yamaguchi, I.; Manabe, T.; Kumagai, T.; Mizuta, S. *Mater. Sci. Semicond. Process.* **2003**, *5*, 207.
(15) Sameshima, T.; Hara, M.; Usui, S. *Jpn. J. Appl. Phys.* **1989**, *28*, 1789.
(16) Bäuerle, D *Laser Processing and Chemistry*; Springer-Verlag: Berlin, 2000.

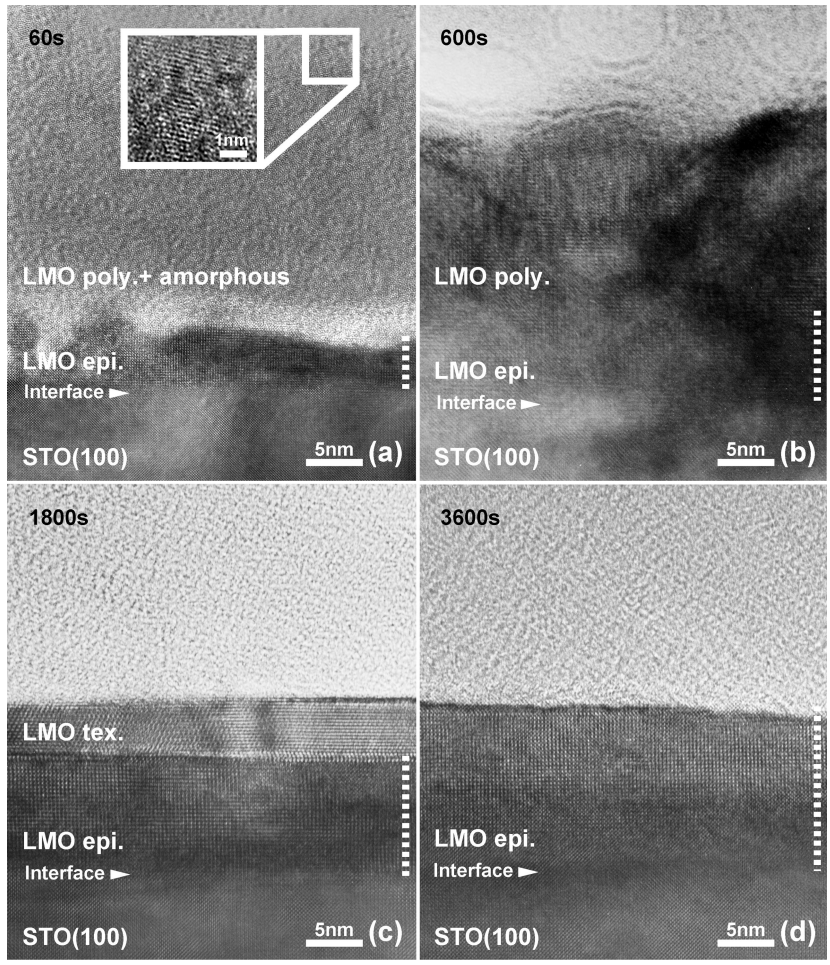

Figure 2. XTEM images for the LMO films on STO(100) prepared by MOD in the furnace at 900 °C for (a) 60, (b) 600, (c) 1800, and (d) 3600 s. The abbreviated terms poly, tex, and epi represent polycrystalline, textured, and epitaxial films, respectively. The dotted line means the epitaxial LMO thickness.

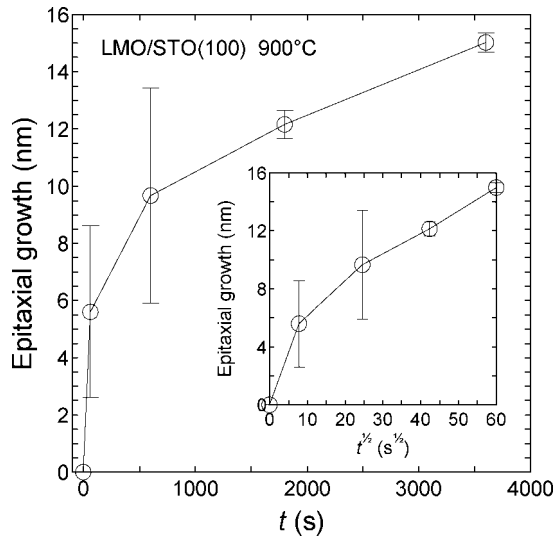

Figure 3. Thickness of epitaxial growth for the LMO films on STO(100) prepared by MOD at 900 °C as a function of the annealing time (t) and the square root of t (inset).

or 20 °C at the bottom of the substrate, and $\kappa(\partial T)/(\partial z) = 0$ at the interfaces (adiabatic condition).

Results and Discussion

Crystal Growth in MOD and ELAMOD Processes. Figure 1a shows FT-IR data for the films after deposition, after drying at 100 °C, and after preheating at 500 °C. The organic components were almost decomposed thorough the drying and preheating processes. From XTEM analysis, the film after preheating at 500 °C was not crystallized at all, and the thickness for the amorphous LMO film was estimated to be about 35 nm combined with the EDX data, as shown in Figure 1b.

Amorphous LMO films on STO(100) after preheating were heated to 900 °C in air (MOD process), and crystal growth under macroscopic heating conditions was evaluated by the XTEM observations. Figure 2 shows the heating time dependence of the XTEM images. For 60 s annealing, LMO started to epitaxially grow on the STO(100) substrate, and simultaneously LMO nanocrystals formed in the amorphous matrix. Epitaxial LMO was continuously grown on the substrate, about 10(4) nm for 600 s, however, polycrystalline LMO was also grown from the nanocrystalline cores as observed in the 60 s annealing sample. The polycrystalline domains aggregated and changed to a dense textured layer on the epitaxial layer after 1800 s, and all domains were finally unified to form the single-crystal epitaxial LMO film at 3600 s.

The thickness of the epitaxial growth was plotted as a function of the annealing time (t) and the square root of t in Figure 3. The epitaxial growth rate of the LMO film in the thermal heating process is not proportional to $\sqrt{t}$. This means that the epitaxial growing rate does not follow a simple

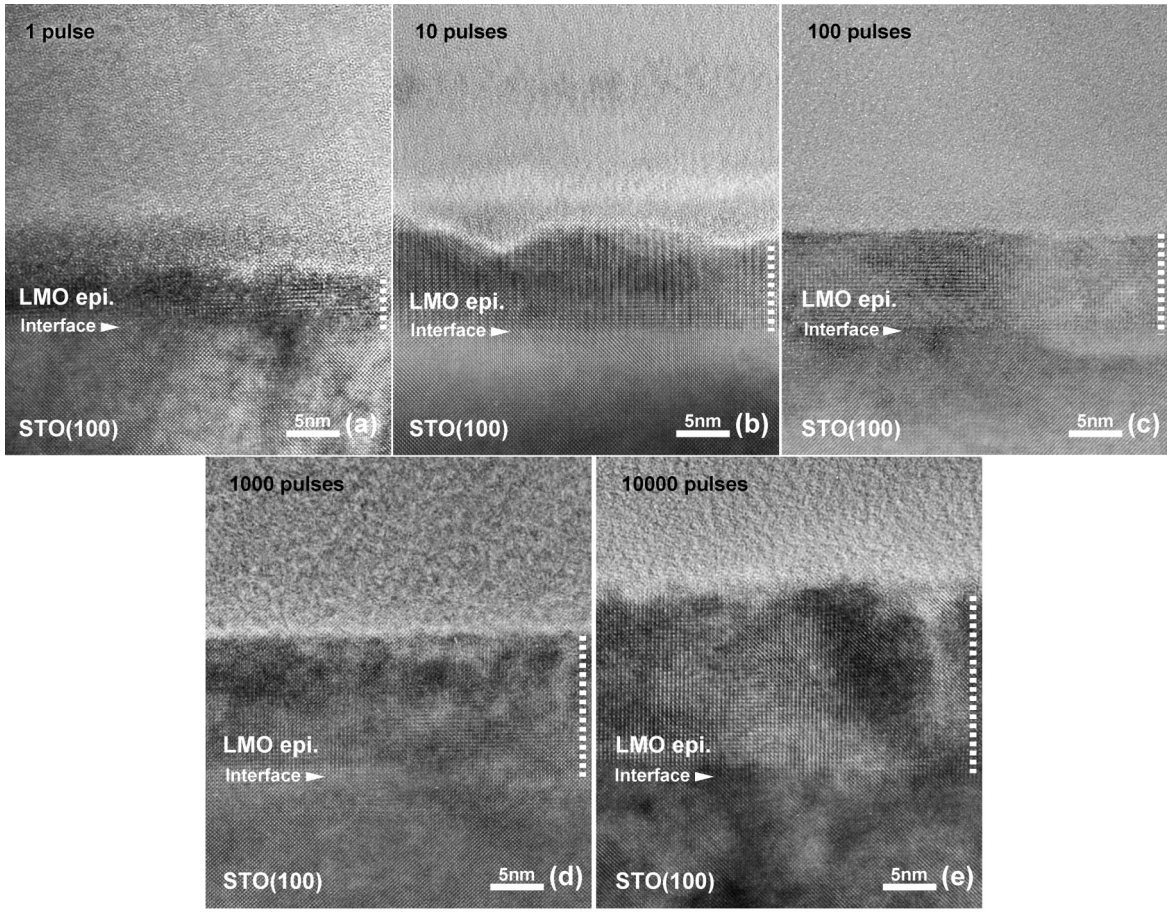

Figure 4. XTEM images for the LMO films on STO(100) prepared by ELAMOD using KrF laser irradiation at a fluence of 100 mJ/cm^2 for (a) 1, (b) 10, (c) 100, (d) 1000, and (e) 10 000 pulse counts at 500 °C. The abbreviation epi represents the epitaxial film. The dotted line means the epitaxial LMO thickness.

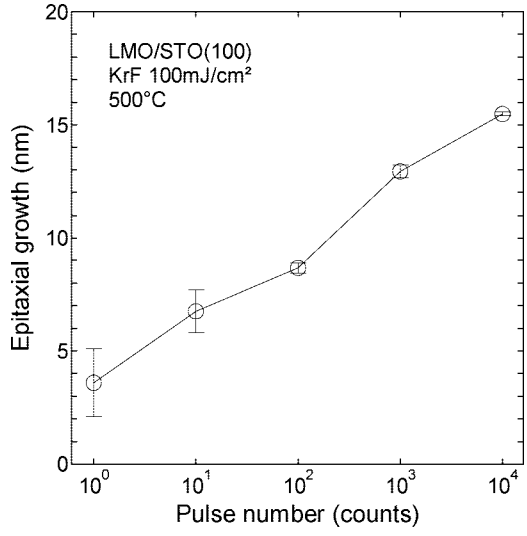

Figure 5. Thickness of epitaxial growth for the LMO films on STO(100) prepared by ELAMOD using KrF laser irradiation at a fluence of 100 mJ/cm^2 at 500 °C as a function of the laser pulse counts.

diffusion model[17] expressed as $d \propto \sqrt{Dt}$ (d, film thickness; D, diffusion coefficient) in this case, because the morphology of the growth interface between the amorphous (polycrystalline) and the epitaxial layers was changed by the strong competition for crystal growth among many crystalline domains in the process of heating.

Next, we consider the epitaxial growth process of the LMO thin films on STO(100) in the ELAMOD. Figure 4 shows the XTEM images after KrF laser irradiation for 1−10 000 pulse counts at 500 °C, and the thickness of epitaxial growth as a function of the number of irradiated laser pulses is plotted in Figure 5. The epitaxial growth of the LMO started from the substrate surface at just 1 laser pulse, and the film thickness was estimated to be about 4(2) nm. After 10 pulses, the LMO was seen to grow epitaxially on the substrate for about 7(1) nm, whereas the interface roughness between the crystalline and amorphous LMO was significantly large, similar to the beginning of the heating process (Figure 2a). This behavior appears to be caused by the inhomogeneity of the heating and ion diffusion due to the mass density fluctuations in the amorphous LMO during the process of rapid shrinkage at the initiation step of the crystallization. The crystallization interface became flat after 100 pulses, and the whole amorphous LMO phase was crystallized and epitaxial on the substrate after 10000 pulses. The final film thickness of the obtained LMO film was estimated to be 15.5(1) nm. In the pulsed laser-assisted process (ELAMOD), it is noteworthy that only epitaxial growth occurred preferentially from the substrate surface, without polycrystalline growth from the amorphous matrix. This indicates that ELAMOD is very effective for forming high-quality epitaxial

(17) Hsieh, J. J. *J. Cryst. Growth* **1974**, *27*, 49.

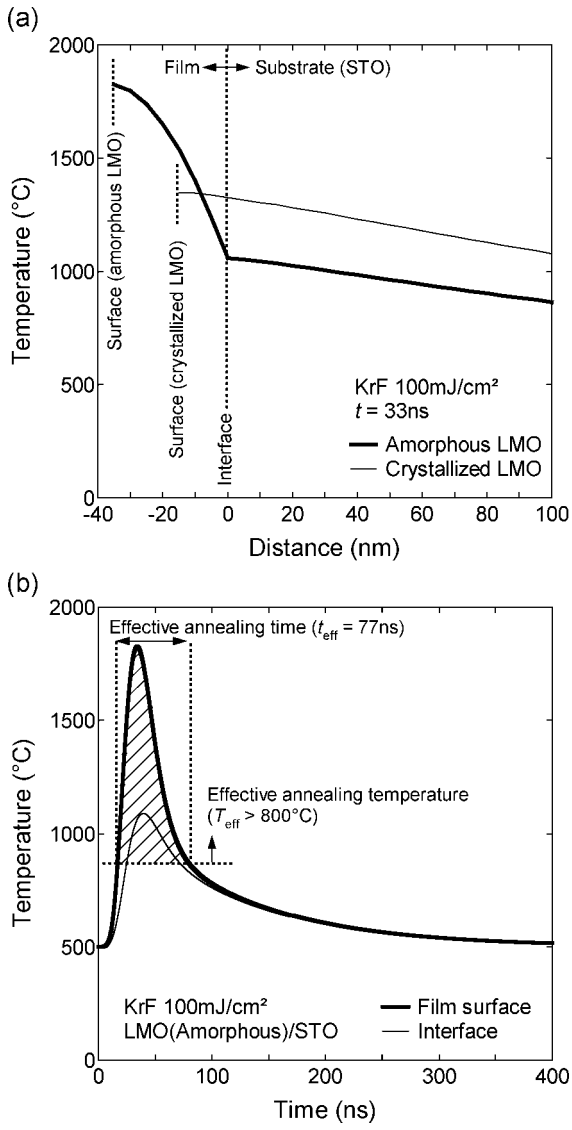

Figure 6. Numerical simulations for (a) distance and (b) time dependence of the temperature variation for the amorphous and crystallized LMO films on the STO substrate under KrF laser irradiation at a fluence of 100 mJ/cm^2. The initial substrate temperature was fixed at 500 °C, and the film thickness for the amorphous and crystallized LMO was 35 and 15 nm, respectively. Effective annealing time (t_{eff} = 77 ns) was calculated by defining the effective annealing temperature (T_{eff}) as 800 °C.

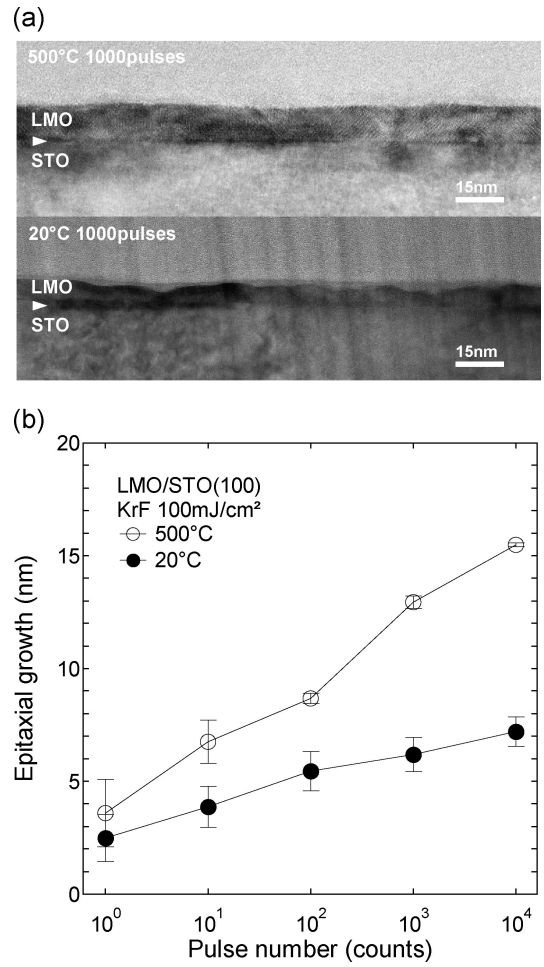

Figure 7. (a) XTEM images for the LMO films on STO(100) prepared by ELAMOD using KrF laser irradiation at a fluence of 100 mJ/cm^2 for 1000 pulses at 20 and 500 °C. (b) Thickness of epitaxial growth for the LMO films on STO(100) at 20 and 500 °C as a function of the laser pulse counts.

films by reducing the dislocations and defects by means of the chemical solution deposition process.

Photothermal and Photochemical Effects on Epitaxial Growth under Pulsed Laser Irradiation. There are mainly two contributions of the excimer laser irradiation for the crystallization of LMO films on single-crystal substrates, photothermal and photochemical effects. The photothermal contribution can be discussed on the basis of theoretical simulations of temperature distributions under the excimer laser irradiation as a function of the depth and the irradiation time. Figure 6a shows the temperature variations for the amorphous and crystallized LMO films under KrF laser irradiation at a fluence of 100 mJ/cm^2 after 33 ns from an incident laser pulse. The initial substrate temperature was fixed at 500 °C, and film thicknesses for the amorphous and crystallized LMO were 35 and 15 nm, respectively. The thermal and physical properties for the numerical simulations are listed in Table 1, according to refs 18−22. The temperature for the amorphous LMO film increased to 1830 °C at the film surface and then decreased to 1050 °C at the interface. After crystallization, the maximum temperature at the film surface (T_{max}) dropped to 1350 °C because of increasing thermal conductivity. The increasing temperature of both the amorphous and crystalline films under the laser irradiation seems to be sufficient for the ion diffusion of LMO through the crystallization process. However, we believe that the LMO films are not crystallized just by the

Table 1. Thermal and Physical Properties for the Numerical Simulations[18−22]

	α (cm^{-1})		*R*				
materials	at 248 nm	at 193 nm	at 248 nm	at 193 nm	κ (W cm^{-1}K^{-1})	ρ (g cm^{-3})	C (J g^{-1}K^{-1})
amorphous LMO	148 000	193 000	0.216	0.172	0.0033	2.77	0.954
crystallized LMO	387 000	445 000	0.119	0.169	0.065	6.50	0.426
$SrTiO_3$	700 000		0.326		0.110	5.11	0.915
$LaAlO_3$	17	80 000	0.204	0.270	0.136	6.70	0.427

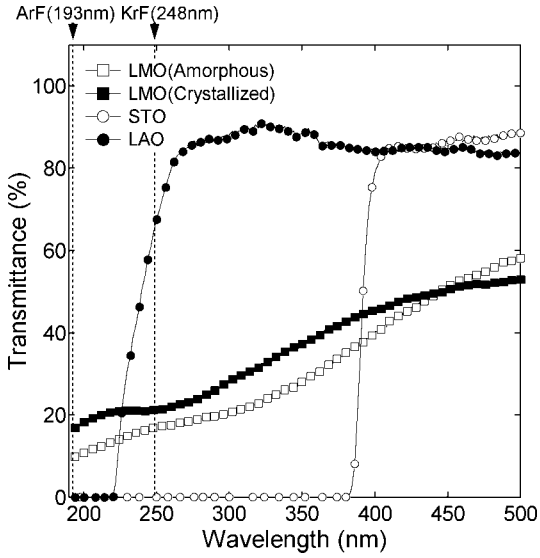

Figure 8. Transmittance spectra of amorphous and crystallized LMO, STO, and LAO as a function of wavelength.

photothermal contribution. If the photothermal effect was dominant for the crystallization of LMO films, the LMO films would be expected to grow not only from the substrate interface, which functions as an active site for crystal nucleation, but also from the film surface that was heated to a significant extent by the laser irradiation. In fact, polycrystalline growth was never observed in the amorphous LMO matrix.

The temperature profiles as a function of time for the LMO films under laser irradiation is shown in Figure 6b. At the film surface, the temperature curve for amorphous LMO shows a maximum at 33 ns (T_{max} = 1830 °C), and is then rapidly cooled to 800 °C at 94 ns. When the effective temperature for the crystallization of the LMO film (T_{eff}) is defined as 800 °C, the effective annealing time (t_{eff}) at the amorphous film surface is estimated to be about 77 ns; it has been reported that LMO was efficiently crystallized above 800 °C in the conventional heating process. This t_{eff} value seems to be small compared to the other cases in which polycrystalline growth of perovskite $CaTiO_3$ and $PbZrO_3$ thin films under pulsed laser irradiation has been observed under the condition that t_{eff} exceeded 200 ns.[7,23] On the basis of these results, crystal nucleation from the amorphous matrix is considered to be difficult by only photothermal heating when t_{eff} is much lower than approximately 200 ns. Threshold analysis of t_{eff} for crystalline nucleation is currently in progress.

XTEM observations of the LMO films prepared by the KrF laser irradiation for 1000 pulses at 20 and 500 °C are shown in Figure 7a. Surprisingly, the LMO film grew epitaxially even at 20 °C, though the crystallized thickness was very thin compared to that of the film prepared at 500 °C. Figure 7b shows the pulse number dependence of the epitaxial growth thickness for the LMO films prepared at 20 and 500 °C. The growth rate of the film prepared at 20 °C was estimated to be less than half-that of the film prepared at 500 °C. From a photothermal temperature simulation, T_{max} of the amorphous LMO film prepared at 20 °C under laser irradiation is estimated to be about 1350 °C (t_{eff} = 32 ns),

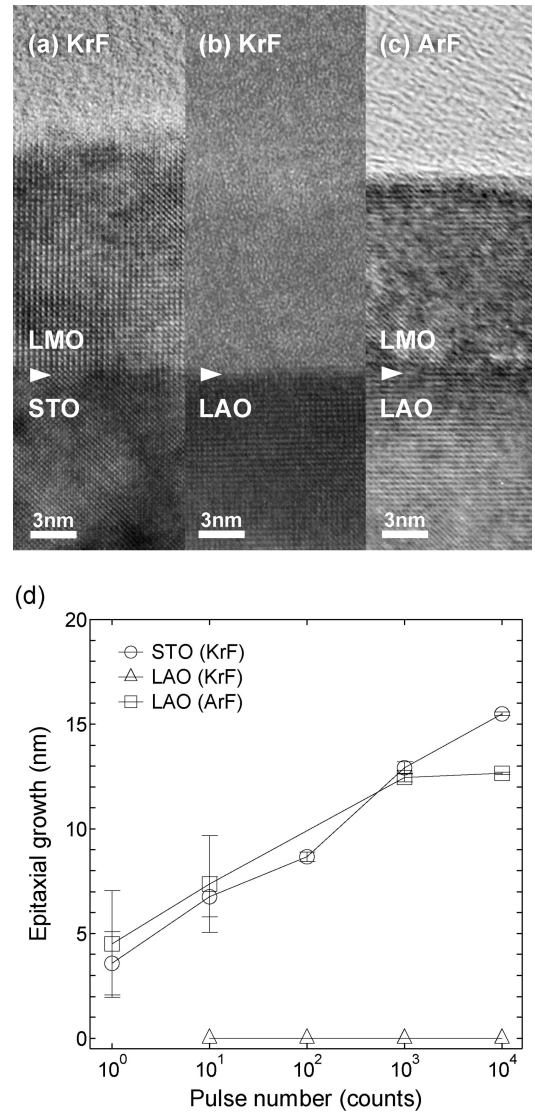

Figure 9. XTEM images for the films (a) on STO(100) under the KrF laser, (b) on LAO(100) under the KrF laser, and (c) on LAO(100) under the ArF laser at a fluence of 100 mJ/cm^2 for 10 000 pulses at 500 °C. (d) Thickness of epitaxial growth for the LMO films as a function of laser pulse counts in each condition.

and the temperature is then rapidly cooled down to near room temperature. The temperature at the substrate surface is also calculated to be 590 °C. The nucleation of LMO crystals seems not to effectively proceed at such a low temperature. Therefore, the photothermal effect in this process is considered not to play a principal role for crystal growth but to just assist ion migration for improving the crystal growing rate.

Figure 8 shows the transmittance spectra for amorphous and crystalline LMO, STO, and LAO as a function of wavelength. Each material showed large absorbance for the ArF laser. However, the KrF laser wavelength was not absorbed by the LAO, whereas the other materials absorbed it well. By focusing on these differences in the optical absorbance, we evaluated the photochemical effect for crystallization of LMO films at the interface between the amorphous LMO and the substrates. Under KrF laser irradiation, the LMO film was epitaxially grown on

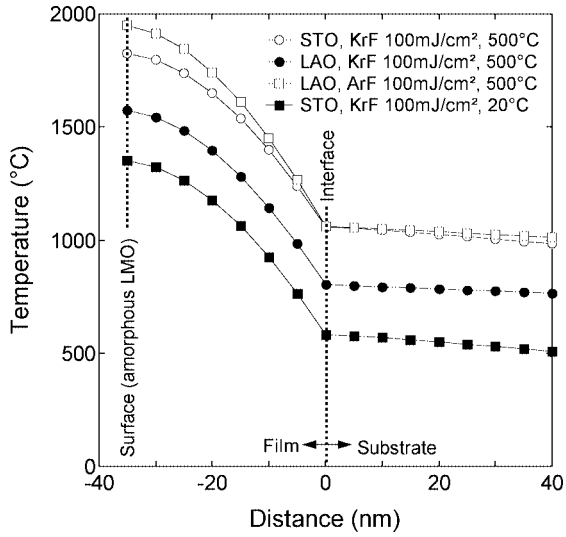

Figure 10. Numerical simulations for distance dependence of temperature variation for the amorphous LMO films on STO and LAO substrates under KrF and ArF laser irradiation at a fluence of 100 mJ/cm^2. The initial substrate temperatures were fixed at 20 and 500 °C, and the film thickness for the amorphous LMO was 35 nm.

STO(100) as mentioned above (Figures 4 and 9a). However, LMO was not crystallized on LAO(100) at all, even when a substantial number of laser pulses was irradiated (10000 pulses) (Figure 9b). The simulated temperature rise under laser irradiations for both substrates as shown in Figure 10 clearly shows that the photothermal heating is not essential to the epitaxial growth: the LMO was crystallized on the STO at much lower temperature compared to the LAO substrate. On the contrary, LMO was epitaxially grown on the LAO(100) substrate under the ArF laser (Figure 9c), whereas laser ablation of the film surface could occur slightly because the temperature would reach close to the melting point of LMO (1900 °C)[24] because of the increasing absorption coefficient of the LMO at 193 nm (Figure 10). The epitaxial growth rates of the LMO films on the STO and LAO substrates were similar to each other in the cases where the irradiated wavelength was absorbed well by the substrates, as shown in Figure 9d. These results clearly show that large optical absorption by the substrates is essential for starting crystal growth for the LMO films, and for LMO to grow epitaxially from the substrate surface. Therefore, we concluded that epitaxial growth in the ELAMOD process is significantly enhanced by optical absorbance of the incident laser wavelength by single-crystal substrates, which can be preferential crystalline nucleation sites.

Epitaxial Growth Mechanism in ELAMOD Process. We can speculate on the detailed mechanism of epitaxial growth in this process as follows. (1) The pulsed laser light is absorbed by a substrate surface that has an ordered lattice, and dangling-bonds on the substrate surface would then be photoactivated for forming chemical bonds. (2) An amorphous material on the substrate starts epitaxial growth if it can form a crystal that has small mismatch with the substrate lattice. When the substrate surface is clean, the epitaxial growth rate will be fastest after the first laser pulse because of small recombination of the photoactivated electrons and holes at the substrate surface. This is demonstrated by the experimental results shown in Figures 7b and 9b; the LMO films showed very rapid growth at the first pulse of about 3−5 nm. (3) The amorphous material continuously crystallized on the epitaxial growth region, which is photoactivated by the laser irradiation. However, the epitaxial growth rate is considered to be lowered by the increasing recombination probability because of the large roughness of the crystallized layer, as shown in images a and b in Figure 4. On the other hand, the growth rate can be increased by photothermal heating, since ion migration would then be enhanced by the pulsed temperature rise. Obviously, furnace heating of a substrate would also cause enhancement of ion diffusion. (4) In the process of laser irradiation, the growth rate would gradually decline, whereas the roughness between the amorphous and crystalline layers is reduced with increasing number of pulses (Figure 4c−e), leading to suppression of recombination of the photoactivated electrons at the reaction interface. The pulsed temperature increase under the laser irradiation decreases with a thinning amorphous layer (the photothermal effect would be intensified in an amorphous phase compared to the crystalline phase, because thermal conductivity of low-density amorphous materials is generally lower than that of a dense crystalline phase, as shown in Figure 6a).

The photoinduced crystallization in the ELAMOD process can thus be explained as indicated above. The start of crystal nucleation and subsequent advance of the crystal growth under laser irradiation is strongly enhanced by the photochemical effect, and is assisted by the photothermal temperature rise in terms of accelerating ion migration. We would like to emphasize that although this concept has been proposed for epitaxial growth on single-crystal substrates, it must have a generality for any crystal growth under laser irradiation in the CSD process; polycrystalline growth from an amorphous matrix would also be enhanced by the photochemical effect, although only the photothermal effect has been discussed so far (the initial nucleation must occur under photothermal heating with sufficient t_{eff}). Polycrystalline films can be efficiently grown by taking into account not only the parameters for the film thickness, T_{max} and t_{eff}, but also the incident laser wavelength for optical absorption of target materials for the photochemical reaction. Thus, the study of epitaxial growth on single-crystal substrates in the ELAMOD process is considered to be a good model for the determination of appropriate preparation conditions for photoinduced crystallization in the CSD process.

Conclusions

We have studied the epitaxial growth of perovskite Manganite LMO on STO(100) and LAO(100) substrates

(18) Jacob, K. T.; Attaluri, M. *J. Mater. Chem.* **2003**, *13*, 934.
(19) Zhou, J. S.; Goodenough, J. B. *Phys. Rev. Lett.* **2006**, *96*, 247202.
(20) Yahia, M.; Batis, H. *Eur. J. Inorg. Chem.* **2003**, *13*, 2486.
(21) Taga, M.; Miyake, H.; Kobayashi, T. *Jpn. J. Appl. Phys.* **1994**, *33*, L1534.
(22) Schnelle, W.; Fischer, R.; Gmelin, E. *J. Phys. D* **2001**, *34*, 846.
(23) Nakajima, T.; Tsuchiya, T.; Kumagai, T. *Appl. Phys. A: Mater. Sci. Process.* **2008**, *93*, 51.
(24) Horyń, R.; Sikora, A.; Bukowska, E. *J. Alloys Compd.* **2003**, *353*, 153.

under excimer laser irradiation in the ELAMOD process. XTEM observations revealed that the LMO was preferentially grown from the substrate surface by the pulsed laser irradiation, and the optical absorbance of the substrates for the irradiated laser wavelength plays an essential role for starting epitaxial growth. This indicates that for the photochemical effect by UV laser irradiation, the photoactivated growth interface strongly enhanced forming chemical bonds, leading to epitaxial growth of LMO. The film temperature under the excimer laser irradiation was estimated using theoretical simulations and a one-dimensional heat equation; the temperature increased up to about 1000−1800 °C after 90 ns. The photothermal temperature rise would contribute to ion migration for crystallization and further the rapid epitaxial growth initiated by the photochemical effect. Thus, the photochemical and photothermal effects are considered to assume the roles of the initiator and enhancer of epitaxial growth respectively under the laser irradiation in the ELAMOD process.

Acknowledgment. We are grateful to H. Ueda at the Institute for Solid State Physics, the University of Tokyo, for his help as well as valuable discussions.

CM801803G